All-fiber sensors for radiation measurements in radiotherapy

All-fiber sensors for radiation measurements in radiotherapy

Aurora Bellone, Massimo Olivero, Wilfried Blanc, Mourad Benabdesselam, Franck Mady, et al.

Aurora Bellone, Massimo Olivero, Wilfried Blanc, Mourad Benabdesselam, Franck Mady, Alberto Vallan, Guido Perrone, "All-fiber sensors for radiation measurements in radiotherapy," Proc. SPIE 12372, Optical Fibers and Sensors for Medical Diagnostics, Treatment and Environmental Applications XXIII, 123720D (6 March 2023); doi: 10.1117/12.2651179

Event: SPIE BiOS, 2023, San Francisco, California, United States

All-fiber sensors for radiation measurements in radiotherapy

Aurora Bellone[a], Massimo Olivero[a], Wilfried Blanc[b], Mourad Benabdesselam[b], Frank Mady[b], Alberto Vallan[a], and Guido Perrone*[a]

[a]Dept. of Electronics and Telecommunications, Politecnico di Torino, 10129 Torino, Italy
[b]Université Côte d'Azur, Nice, France

ABSTRACT

The paper presents the development and investigation of distributed and a quasi-distributed fiber optic sensors for the real-time monitoring of radiations during cancer treatments. Both sensors rely on ad-hoc developed nanoparticle-doped optical fibers with enhanced sensitivity to radiation. The distributed sensor is interrogated with an OFDR-based instrument and allows the reconstruction of the spatial dose distribution along the fiber. The quasi-distributed sensor is implemented through fiber Bragg gratings inscribed with a femtosecond laser in the few-mode section of a single mode-multi mode-single mode interferometer.

Keywords: Radiation dose measurement, Optical fiber sensors, Distributed fiber sensors, Fiber Bragg grating sensors, Interferometric sensors.

1. INTRODUCTION

Ionizing radiation are widely employed in the medical field both for diagnosis (x-rays, computed tomography scan, etc.) and for treatments (radiotherapy), especially of tumors.[1] Focusing in particular on the radiotherapy, it is important to measure the dose correctly to effectively kill cancerous cells, while avoiding unnecessary damage to normal cells, particularly in the case of ultra-high dose radiotherapy, the so-called FLASH therapy. Adjuvant therapy doses typically require up to 60 Gy and conventional radiotherapy techniques divide it into multiple doses over a period of months. This leads to about 2 Gy dose per treatment, delivered at a very low dose rate, in the order of 0.02 Gy/s to 0.03 Gy/s. On the contrary, FLASH therapy relies on very high dose rate of about 40 Gy/s delivered for less than a second.[3] Given the extremely high dose rate, achieving optimal outcomes would require an accurate quantification of the delivered radiation dose and of its spatial distribution in real-time and this, of course, without introducing perturbations in the ongoing treatment.

Today available measurement devices are not capable of satisfying these requirements. Indeed, while the dose value can be evaluated with various approaches, such as Geiger-Müller counters and ionization chambers or scintillators,[2] the measurement can done in practice only in phantoms, prior to the actual treatment. Even worst is the situation for the evaluation of the spatial distribution of the radiation in the target volume because it is typically done only qualitatively since the most common approach is to use GafChromic (GaF) films, which contain a special dye that changes its optical density upon exposure to radiation.[4]

A solution to overcome these limitations can come for optical fibers because they provide an attractive technological platform for the realization of new ionizing radiation sensors that are capable of real time detection of both the dose rate and the spatial distribution. In general, fiber optics is known for allowing the development of biomedical sensors characterized by a high sensitivity combined with a minimal invasive impact, an excellent biocompatibility, and the intrinsic impossibility of electrocution. The reduced invasiveness given by the small dimensions of the fibers is particularly relevant in radiotherapy monitoring because it means that a negligible shadow is generated. Besides, being all dielectric, fiber optic sensors do not affect magnetic resonance imaging. Unfortunately, standard silicate optical fibers for telecom applications exhibit little sensitivity to ionizing radiations. This issue can addressed by developing ad-hoc silicate fiber, like those doped with aluminum nanoparticles, that for their behavior can be called Enhanced Backscattering Fibers (EBFs)[5,6] .

*guido.perrone@polito.it; phone +39 011 0904146; fax +39 011 0904099; www.polito.it

Optical Fibers and Sensors for Medical Diagnostics, Treatment and Environmental Applications XXIII,
edited by Israel Gannot, Katy Roodenko, Proc. of SPIE Vol. 12372,
123720D · © 2023 SPIE · 1605-7422 · doi: 10.1117/12.2651179

The paper reports on the investigations of two types of optical fiber dosimeters made with different EBFs:[7] i) a fully distributed sensing system that relies on an Optical Frequency Domain Reflectometer (OFDR) to evaluate the spatial distribution of the ionizing radiation and ii) a point (extendable to quasi-distributed) sensing system that makes use of a combination of an interferometric sensor in the form a Single mode-Multimode-Single mode (SMS) structure with a Fiber Bragg Grating (FBGs).

2. SETUP AND METHODS

Both the OFDR distributed and the SMS/FBG quasi-distributed sensing arrangements are based on a custom EBF, a silicate fiber drawn from a glass preform fabricated by Modified Chemical Vapor Deposition (MCVD), whose core is properly doped with nanoparticles that enhance the Rayleigh backscattering. The effectivity of this fiber has already been proved, showing that the backscattering signature along the fiber changes under exposure to radiations.[8–10] In particular, while this change produces a limited Radiation Induced Attenuation (RIA), the Radiation Induced Refractive Index Change (RRIC) is considerable and can be successfully detected both sensing schemes.

The distributed sensing system relies on a Luna OBR4600, an OFDR based on a swept wavelength laser, a Mach-Zender interferometer and two photodetectors. The reference arm of the Mach-Zender is fixed, whilst the fiber sensor modifies the propagation on the sensing arm. The resulting interference signal embeds information on amplitude, phase and position of the reflective events along the fiber. The achievable spatial resolution can be below hundred micrometers, although the higher the requested resolution, the longer it takes to perform the measurement. This limits the applicability of this approach because in some types of radiotherapies, such as in FLASH therapies, the irradiation time is comparable, or even shorter, than the time required to perform the data acquisition and processing. In this case, the quasi-distributed system based on SMS/FBG may be more appropriate since the measure can be performed within milliseconds with a fast FBG interrogator.

The SMS/FBG sensor considered in this work is sketched in Fig. 1 and consists of an FBG is inscribed in the multimode section of an SMS fiber structure.[?]

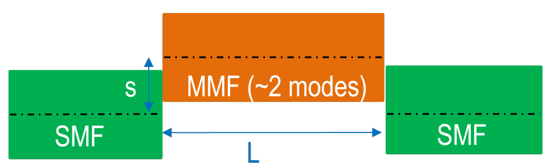

Figure 1: Schematic representation of the interferometric sensor SMS in which an FBG has been inscribed in the multimode section. SMF: standard single mode fiber; MMF: multimode fiber that supports the propagation of two modes that in this case is an enhanced backscattering fiber (EBF).

The fabrication of the SMS/FBG is performed by splicing a short EBF between two SMF patchcords, with a special fusion splicing recipe in which an offset of 3 µm to 5 µm between the core axes is set to excite both the fundamental and the first higher order mode. The structure then works as an all-fiber Mach-Zender interferometer. The EBF section also contains a femtosecond-written FBG to introduce a complementary sensing mechanism that can be exploited to compensate spurious phenomena such as mechanical strain and temperature variations. The FBG is inscribed wavelengths in the so-called third optical communications window by Point-by-Point technique (PbP) using a around 515 nm laser source. The PbP inscription easily allows obtaining any spectral response because the periodic perturbation in the core that forms the grating is generated by focusing the writing beam in a sequence of points at predefined positions along the fiber core axis. The result of the combination of an SMS and an FBG sensor is reflection spectra that exhibits a periodic pattern given by the SMS structure and a Bragg peak produced by the FBG. Both shift under X-ray exposure because of the RRIC phenomenon, with the SMS sensitivity being higher than that of the FBG.

The distributed and quasi-distributed sensors have been exposed to X-rays in a shielded radiation chamber, according to the schematic of Fig. 2. The distance of the sensing fibers from the X-ray emitter is adjusted to control the delivered dose and the exposed length. For this work, most of the experiments were performed either at high dose rates (700 Gy/min, a value comparable with those used in FLASH therapies, although maintained for longer times to allow using the distributed sensing system) or at low dose rates (2 Gy/min, a value close to standard therapeutic values).

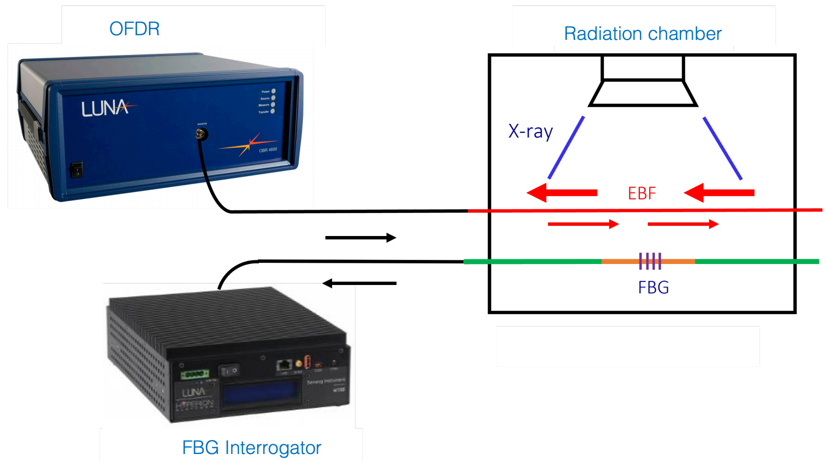

Figure 2: Schematic representation of the measurement setup, in which the distributed sensor (i.e., the EBF) and the quasi-distributed sensor (SMS/FBG) are exposed to X-rays in radiation chamber and remotely interrogated by the OFDR (Luna OBR 4600) and the FBG interrogator (Luna Hyperion si155), respectively.

An automatic routine in LabView™ has been on-purpose implemented to acquire the backscattering signal from the OBR in a configuration denoted as "sensing mode" at the maximum acquisition rate. In sensing mode, an initial reference trace is saved before the beginning of the irradiation; then, all the following acquisitions performed during X-ray exposure are processed with the reference to extract the spectral shift, expressed in GHz, of the backscattering signature along the fiber, which is proportional to the RRIC. The instrument requires the setting of three parameters, namely the gauge length, the sensor spacing and the sensing range. Since the exposed fiber can be regarded as a highly dense FBG array, the gauge length corresponds to the equivalent length of these "virtual" FBGs, the sensor spacing parameter to the separation between two subsequent equivalent FBGs, and the sensing range as the length of the FBG array. The values set for the results hereby presented were: 0.16 mm for the sensor spacing (the lowest value), 30 mm for the gage length, and 1 m for sensing range. These parameters led to an acquisition time of 10 s (0.1 Hz).

In the case of quasi-distributed sensing with the SMS/FBG sensor and the FBG interrogator, the measurement rate is not an issue and can be as fast as 10 Hz, or even higher, and the recording of the data can be performed by the proprietary software of the instrument.

3. RESULTS

The setup and the exposure procedure are the same for both sensor types. For practical reasons in the various tests the x-ray emitter has been always driven at constant current and the delivered dose has been controlled by changing the distance between the emitter and the sensor. Clearly, this also changed the length of the fiber exposed to the radiation.

Different dose rates from 700 Gy/min to 2 Gy/min have been considered, but the results hereby reported and are for the high dose of 700 Gy/min (corresponding to 0.2 pm/Gy) only. Two different EBFs – labelled as S22-01-P1 and R08-01 – are considered: the first fiber is an Er-doped silicate fiber with lanthanum nanoparticles, while the R08-01 contains aluminum as the radiation-sensitive dopant.

3.1 S22-01-P1

For the S22-01-P1, only the SMS sensing structure and the fully distributed sensor have been tested. The behavior of the interferometric sensor is shown in Fig. 3, from which it is evident the high sensitivity that reaches 150 pm/min.

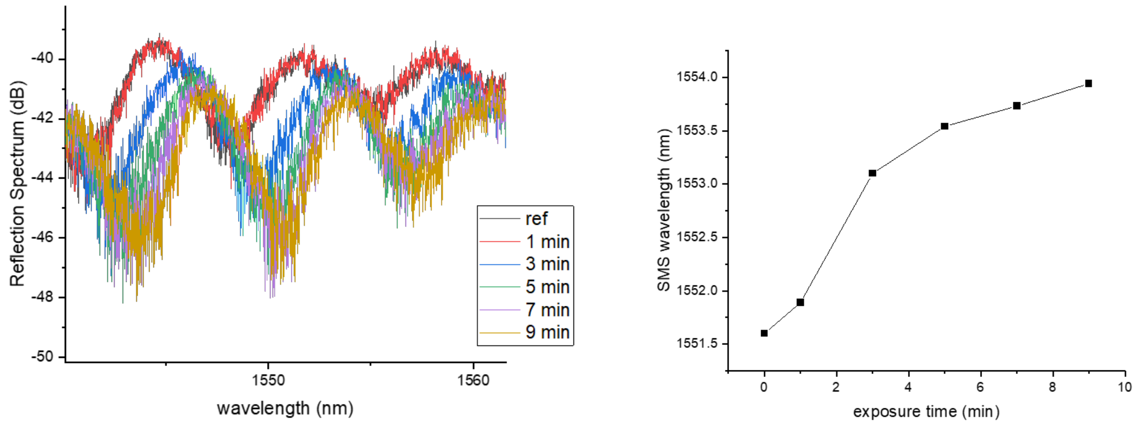

(a) (b)

Figure 3: Response of interferometric sensor made with the S22-01-P1 EBF: (a) spectral response and (b) its relative wavelength shift with the increase of the delivered dose.

Measuring the EBF with the OFDR interrogator, the acquired signal is the spectral shift along the length of the sensor. The section exposed to the X-rays beam is evident in the upper Fig. 4 because it coincides with the notch that becomes deeper and deeper as the delivered dose increases. The bottom part of Fig. 4 reports the evolution in time of the spectral shift for the same dose rate. The sensitivity is 0.5 pm/min.

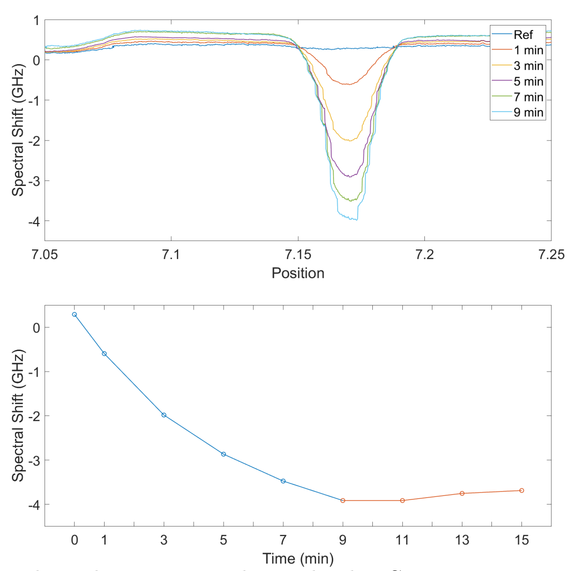

Figure 4: Response of the distributed sensor made with the S22-01-P1 EBF: (upper) spectral shift versus position along the fiber and (lower) it relative evolution with the increase of the delivered dose (the change of color corresponds to the behavior after the source has been turned off).

3.2 R08-01

For the fiber R08-01 the behavior of an FBG and of a distributed sensor are reported. In particular, Fig. 5 shows the spectral variation and the shift of the Bragg peak in time as the delivered dose increases, while Fig. 6 shows the the spectral shift as measured by the OFDR instrument.

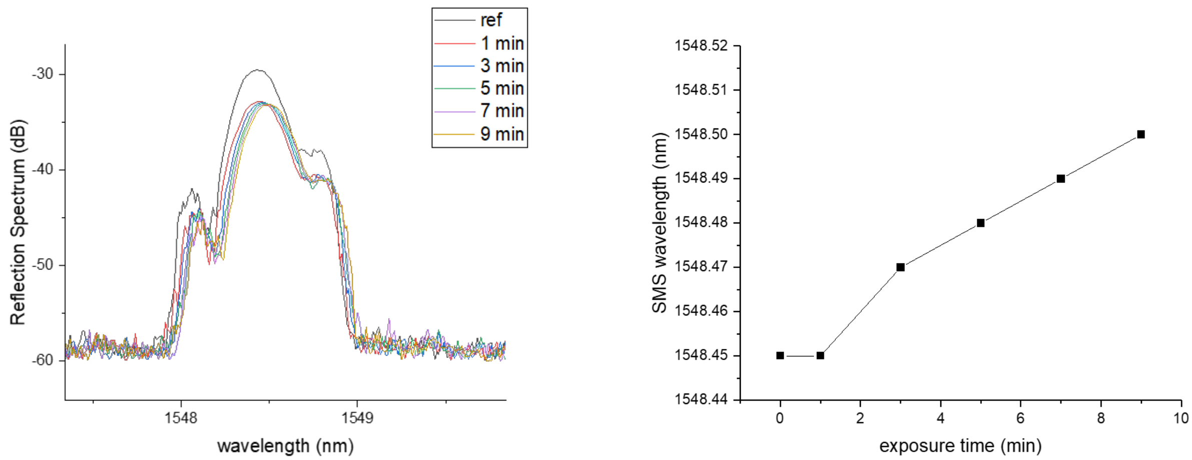

(a) (b)

Figure 5: Spectrum of the FBG inscribed in the S26-01-P1 sensor (a) and its relative shift with the increasing of the delivered dose (b).

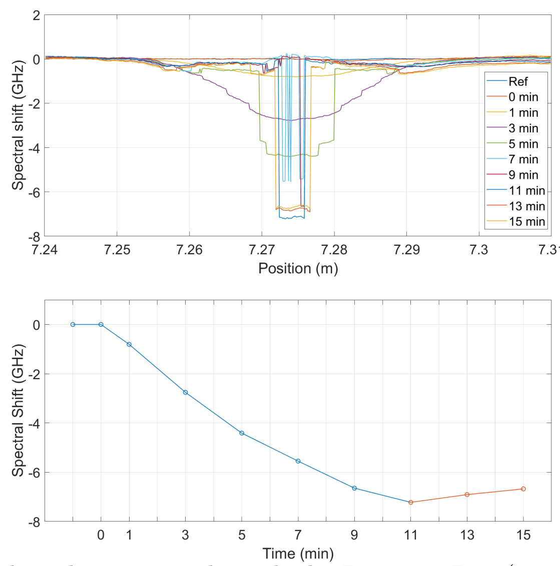

Figure 6: Response of the distributed sensor made with the R08-01 EBF: (upper) spectral shift versus position along the fiber and (lower) it relative evolution with the increase of the delivered dose (the change of color corresponds to the behavior after the source has been turned off).

4. CONCLUSIONS

Differently special enhanced backscattering fibers have been investigated as radiation sensors with two sensor architectures, namely interferometric (SMS, possibly combined with an FBG to introduce compensation capabilities, although this option is not discussed here) and distributed (a span of EBF interrogated by OFDR).

The two fibers are silicate fibers, respectively doped with La and Al nanoparticles, and the have been exposed a similar irradiated dose. Analyzing the results reported in Fig. 4 and in Fig. 6 it is evident that they exhibit a slight difference in the maximum spectral shift and a more marked difference in the recover phase, which the behavior once the X-ray source is turned off. Both fibers present a bleaching phenomenon, more rapid for the metal containing fiber (R08-01).

As for the SMS/FBG sensors, the results reported in Fig. 3 and in Fig. 5 confirmed the higher sensitivity of interferometric version, already shown in other papers,[10] which will be exploited in future works to introduce a compensation for the parasitic effects.

The obtained results demonstrate that the developed EBFs are promising to develop radiations sensors to be interrogated with different sensing architectures in dependence of the specificity of the dose rate of radiotherapy protocol.

REFERENCES

[1] Mythreyi, B., "Trends in the utilization of medical procedures that use ionizing radiation," Health Physics 95, 612–627 (2008).

[2] Hu, Y., Qin, Z., et al., "Characterization of fiber radiation dosimeters with different embedded scintillator materials for radiotherapy applications," Sensors and Actuators A: Physical 269, 188–195 (2018).

[3] Ramish, A. M., Mahbubur, R., Rongxiao, Z., et al., "Dosimetry for FLASH radiotherapy: a review of tools and the role of radioluminescence and Cherenkov emission, " Frontiers in Physics 8, 328 (2020).

[4] Micke, A., Lewis, D. F., Yu, X., "Multichannel film dosimetry with nonuniformity correction," Med. Phys. 38, 2523–2534 (2011).

[5] Westbrook, P. S., Feder, K. S., et al., "Kilometer length, low loss enhanced back scattering fiber for distributed sensing," 25th Optical Fiber Sensors Conference (OFS), 1–5 (2017).

[6] Lu, Z., Robine, T., et al., "Toward engineered nanoparticle-doped optical fibers for sensor applications," Frontiers in Sensors 2, (2022).

[7] Beccaria, A., Bellone, A., et al. "Temperature monitoring of tumor hyperthermal treatments with optical fibers: comparison of distributed and quasi-distributed techniques," Optical Fiber Technology 60, 102340 (2020).

[8] Blanc, W., Mauroy, V., Nguyen, L., et al., "Fabrication of rare earth-doped transparent glass ceramic optical fibers by modified chemical vapor deposition," Journal of the American Ceramic Society 94, 2315–2318 (2011).

[9] Blanc, W., Martin, I., et al., "Compositional changes at the early stages of nanoparticles growth in glasses," The Journal of Physical Chemistry C 123, 29008–29014 (2019).

[10] Olivero, M., Mirigaldi, A., et. al., "Distributed X-ray dosimetry with optical fibers by optical frequency domain interferometry," IEEE Transactions on Instrumentation and Measurement 70, 1–9 (2021).

[11] Olivero, M., Vallan, A., Orta, R., Perrone, G., "Single-mode–multimode–single-mode optical fiber sensing structure with quasi-two-mode fibers," IEEE Transactions on Instrumentation and Measurement 67, 1223–1229 (2017).